Regulation of a plant aquaporin by a Casparian strip membrane domain protein-like

Chloé Champeyroux, Jorge Bellati, Marie Barberon, Valerie Rofidal, Christophe Maurel, Veronique Santoni

Santoni Veronique (Orcid ID: 0000-0002-1437-0921)

Amtmann Anna (Orcid ID: 0000-0001-8533-121X)

Title

Regulation of a plant aquaporin by a Casparian strip membrane domain protein-like

Running title

Plant aquaporin regulation

Authors

Chloé Champeyroux[1], Jorge Bellati[1], Marie Barberon[2], Valérie Rofidal[1], Christophe Maurel[1], Véronique Santoni[1,3]

Institute

[1]BPMP, Univ Montpellier, CNRS, INRA, Montpellier SupAgro, Montpellier, France

[2] Department of Botany and Plant Biology, Quai Ernest-Ansermet 30 Sciences III CH-1211 Genève 4 Switzerland

[3]**Corresponding author**

Véronique Santoni

BPMP, Univ Montpellier, CNRS, INRA, Montpellier SupAgro, F-34060 Montpellier cedex 2, France. Tel: 33-4-99 61 20 20. E-mail: veronique.santoni@inra.fr

This article has been accepted for publication and undergone full peer review but has not been through the copyediting, typesetting, pagination and proofreading process which may lead to differences between this version and the Version of Record. Please cite this article as doi: 10.1111/pce.13537

Keywords

Aquaporin, Casparian strip membrane domain protein-like, root hydraulics, suberization

Abbreviations

ABA, abscisic acid; CASPL, CAsparian Strip membrane domain Protein-Like; CSD, Casparian Strip membrane Domain; FLIM, Fluorescence Lifetime Imaging Microscopy; FRET, Förster Resonance Energy Transfer; IP, immuno-purification; J_s, solute flow through the root, $Lp_{r\text{-}h}$, root hydrostatic hydraulic conductivity; $Lp_{r\text{-}o}$, root osmotic hydraulic conductivity; OST1, Open Stomata 1; PIP, Plasma membrane Intrinsic Protein; PIP2;1-AA, PIP2;1 form with Ser-to-Ala mutations at Ser280 and Ser283; PIP2;1-DD, PIP2;1 form with Ser-to-Asp mutations at Ser280 and Ser283; SIRK1, Sucrose Induced Receptor Kinase 1; TSPO, Tryptophan-rich Sensory Protein/translocator.

Abstract

The absorption of soil water by roots allows plants to maintain their water status. At the endodermis, water transport can be affected by initial formation of a Casparian strip, and further deposition of suberin lamellas and regulated by the function of aquaporins. Four Casparian strip membrane domain protein-like (CASPL) (CASPL1B1, CASPL1B2, CASPL1D1 and CASPL1D2) were previously shown to interact with PIP2;1, (Bellati et al. 2016). The present work shows that CASPL1B1, CASPL1B2 and CASPL1D2 are exclusively expressed in suberized endodermal cells, suggesting a cell-specific role in suberization and/or water transport regulation. When compared to wild-type plants, and by contrast to *caspl1b1*caspl1b2* double loss-of-function, *caspl1d1*caspl1d2* double mutants showed, in some control or NaCl stress experiments and not upon ABA treatment a weak enlargement

of the continuous suberization zone. None of the mutants showed root hydraulic conductivity (Lp_r) phenotype, whether in control, NaCl or ABA treatment conditions. The data suggest a slight negative role for CASPL1D1 and CASPL1D2 in suberization under control or salt stress conditions, with no major impact on whole root transport functions. At the molecular level, CASPL1B1 was able to physically interact with PIP2;1, and potentially could influence the regulation of aquaporins by acting on their phosphorylated form.

Summary Statement

The absorption of soil water by roots allows plants to maintain their water status. At the endodermis, water transport can be affected by initial formation of a Casparian strip, and further deposition of suberin lamellas and regulated by the function of aquaporins. Four Casparian strip membrane domain protein-like (CASPL) (CASPL1B1, CASPL1B2, CASPL1D1 and CASPL1D2) were previously shown to interact with PIP2;1, (Bellati et al. 2016). The present work shows that CASPL1B1, CASPL1B2 and CASPL1D2 are exclusively expressed in suberized endodermal cells, suggesting a cell-specific role in suberization and/or water transport regulation. When compared to wild-type plants, and by contrast to caspl1b1*caspl1b2 double loss-of-function, caspl1d1*caspl1d2 double mutants showed, in some control or NaCl stress experiments and not upon ABA treatment a weak enlargement of the continuous suberization zone. None of the mutants showed root hydraulic conductivity (Lpr) phenotype, whether in control, NaCl or ABA treatment conditions. The data suggest a slight negative role for CASPL1D1 and CASPL1D2 in suberization under control or salt stress conditions, with no major impact on whole root transport functions. At the molecular level, CASPL1B1 was able to physically interact with PIP2;1, and potentially could influence the regulation of aquaporins by acting on their phosphorylated form.

1 - INTRODUCTION

The absorption of soil water by roots is crucial for plants to maintain their water status. During radial transport from the soil to the root xylem, water flows along cell wall structures (apoplastic path) or from cell to cell, along cytoplasmic continuities formed by plasmodesmata (symplastic path) or across cell membranes (transcellular path). At the endodermis, water transport is limited by cell wall modifications. In vascular plants, the Casparian strip, a ring-like cell wall structure made of lignin, blocks the apoplastic passive flow of molecules in the endodermis (Geldner, 2013 for review). This cell layer undergoes a second stage of differentiation with the deposition of suberin lamellas between the primary cell wall and the plasma membrane, on either side of the Casparian strip, thereby covering the entire cell surface (Geldner, 2013 for review) and limiting the diffusion of molecules through the plasma membrane (Barberon et al. 2016). This process occurs first in isolated endodermal cells defining a patchy suberization zone, and thereafter in every endodermal cell, resulting in a continuous suberization zone. The only exceptions are "passage cells", some endodermal cells adjacent to xylem poles, that facilitate diffusion of water and solutes to the stele (Andersen et al. 2018).

Casparian strip (Pfister et al. 2014) and suberin lamellas (Ranathunge & Schreiber, 2011, Yadav et al. 2014) are not the only components that determine the root water permeability (root hydraulic conductivity; L_{pr}). Depending on the developmental stage of the plant, its nutritional or hormonal status, or multiple environmental cues, L_{pr} is largely dependent on aquaporins (Di Pietro et al. 2013; Maurel et al. 2015). Aquaporins are 25-30 kDa transmembrane proteins facilitating the diffusion of water and small neutral solutes across cell membranes (Kaldenhoff et al. 2008; Maurel et al. 2008; Tornroth-Horsefield et al.

2006). In *Arabidopsis,* thirty five homologs comprised in four homology subclasses have been identified. The Plasma membrane Intrinsic Proteins (PIPs) (with 13 isoforms further subdivided in the PIP1 and PIP2 subgroups) are the most abundant aquaporins in the plasma membrane (Johanson & Gustavsson, 2002; Quigley et al. 2002). The response of plant roots to environmental and hormonal stimuli is mediated through long-term transcriptional control of aquaporins, and on a shorter term through multiple post-translational modifications and protein-protein interactions. Aquaporin phosphorylation is a significant component of plant responses to stresses [(Santoni, 2017) for review]. For instance, PIPs show a conserved phosphorylation site in their first cytosolic loop (loop B) and, in PIP2 isoforms, multiple phosphorylations in adjacent sites of their C-terminal tail regulate their activity and targeting to the plasma membrane [(Santoni, 2017) for review].

Protein-protein interaction is another post-translational process that can interfere with the intrinsic activity of PIPs, the targeting to their destination compartment, or their stability. For instance, hetero-tetrameric interactions between PIP1s and PIP2s were shown to be required for *in planta* trafficking of PIP1s to the plasma membrane (Chen et al. 2013; Li et al. 2013; Zelazny et al. 2007). The targeting of some PIP2s to the plasma membrane is also facilitated by their interaction with syntaxins, a family of proteins involved in vesicle trafficking (Besserer et al. 2012; Hachez et al. 2014). In addition, the tryptophan-rich sensory protein/translocator (TSPO), a multi-stress regulator that is transiently induced by abiotic stresses and especially osmotic stress, and degraded through a selective autophagic pathway, physically interacts with PIP2;7 and induces its degradation (Hachez et al. 2014). PIP2;1 also functionally interacts with Rma1H1, a membrane-anchor E3 ubiquitin ligase homolog, induced by osmotic stresses, to regulate aquaporin cellular levels through internalization and endoplasmic reticulum retention (Lee et al. 2009). Sucrose Induced

Receptor Kinase 1 (SIRK1) was shown to directly modulate the C-terminal phosphorylation of PIP2;4 and to stimulate water transport in a sucrose deficiency and resupply context (Wu et al. 2013). In contrast, the SnRK2.6 (Open Stomata 1, OST1) protein kinase phosphorylates Ser121 in the loop B of PIP2;1, thereby activating the aquaporin in response to abscisic acid (ABA) and flg22 treatments (Grondin et al. 2015; Rodrigues et al. 2017). A recent study also revealed that harpin Hpa1, a bacterial effector, can interact with PIP1;4 and promote water transport through *Arabidopsis* tissues (Li et al. 2015). While these examples show that a significant number of PIPs protein interactants have been identified individually, many others remain to be discovered. For instance, a recent study based on an extensive affinity purification procedure of PIPs combined with mass spectrometry identification of proteins has revealed more than 300 protein interactants for PIP2;1 (Bellati et al. 2016). Although the functional effects of most of these interactants remain to be determined, this study revealed that two of them, the receptor like kinases RKL1 and Feronia stimulate and inhibit PIP2;1, respectively (Bellati et al. 2016). Four Casparian strip membrane domain proteins-like [CASPL1B1 (At5g44550), CASPL1B2 (At4g20390), CASPL1D1 (At4g15610) and CASPL1D2 (At3g06390)], were also identified among the PIP2;1 protein interactants (Bellati et al. 2016). These proteins of unknown function belong to the CASPL family, with 39 members in *Arabidopsis* (Roppolo et al. 2014), including the CASPs. CASPs are four-membrane-span proteins mediating the deposition of Casparian strips in the endodermis by recruiting the lignin polymerization machinery to the Casparian strip membrane domain (CSD) (Doblas et al. 2017 for review). Whereas *CASPs* are exclusively expressed in the endodermis, *CASPLs* can be expressed in other tissues (Roppolo et al. 2014) and thereby could act as organizers of other types of cell wall-modifying machineries (Roppolo et al. 2014).

In the present work, we went on to characterize the tissular expression pattern of CASPL1B1, CASPL1B2, CASPL1D1 and CASPL1D2, and assessed their effect on cell wall modifications. Due to their putative role in PIP regulation, the main objective was to evaluate the interference of CASPLs with root water transport and aquaporin function.

2 - MATERIAL AND METHODS

2.1 - Constructs

The constructs for oocyte expression (pGEM-GWC-*PIP2;1,* pGEM-GWC-*PIP2;1-S280A-S283A*, pGEM-GWC-*PIP2;1-S280D-S283D*) and FLIM experiments (pB7WGR2-*PIP2;1*, pB7WGR2-*PIP2;1-S280A-S283A*, pB7WGR2-*PIP2;1-S280D-S283D*) have already been described (Bellati et al. 2016). All other constructs except *pCASPL1D1::CASPL1D1-GFP* and *pCASPL1D2::GFP-CASPL1D2* were obtained using the Gateway® cloning technology (Invitrogen) according to the manufacturer's instructions and checked by sequencing. Promoter sequences (*pCASPL1B1*, *pCASPL1B2s*, *pCASPL1D1*, *pCASPL1D2*) were defined as the Col-0 genomic DNA sequence upstream of the starting codon of the gene of interest *i.e. CASPL1B1* (At5g44550), *CASPL1B2* (At4g20390), *CASPL1D1* (At4g15610) and *CASPL1D2* (At3g06390), up to the end of the open reading frame of neighboring gene *i.e.* At5g44555 for *CASPL1B1* (length 1634 bp), At4g20380 for *CASPL1B2* (length 629 bp), At4g15590 for *CASPL1D1* (length 1906 bp) and At3g06400 for *CASPL1D2* (length 1358 bp). Regarding *CASPL1B2*, a longer promoter fragment (*pCASPL1B2l*) corresponding to the 2kb genomic DNA sequence upstream *CASPL1B2* was also cloned. The promoter sequences and the Col-0 cDNA of *CASPL1B1* and *CASPL1D2* were amplified by PCR (iProof™ High-Fidelity PCR kit, Biorad) using the primers described in Table S1. A second PCR using AttB1 or AttB1' and AttB2 or AttB2' primers

(Table S1) allowed the addition of attB recombination sites, and subsequent cloning into pDonor207 (Invitrogen) vector using a Gateway® BP Clonase enzyme mix (Invitrogen). The sequences were then transferred to different destination vectors using a Gateway® LR Clonase enzyme mix (Invitrogen). For tissue-specific expression analysis, promoter sequences were cloned into pGWB533 vector to be fused with the *β-glucuronidase* (*GUS*) coding sequence (Nakagawa et al. 2007). For FLIM experiments, cDNA sequences were cloned into pB7WGF2 or pB7FWG2 vectors to allow fusion of the GFP to the N- or C-terminus of the protein of interest, respectively (Karimi, Inze & Depicker, 2002). pENTR/$_{D}$-TOPO-*AGG1* (Martiniere et al. 2012) was used to clone *AGG1* (At3g63420) in pB7RWG2 thereby fusing RFP to the N-terminus of AGG1. For expression in *Xenopus* oocytes, cDNAs were cloned into pGEM-GWC, a pGEM-HE vector (Liman et al. 1992) containing a Gateway® cassette between the 5' and 3' UTR from a ß-globin gene of *Xenopus*.

pCASPL1D1::CASPL1D1-GFP and *pCASPL1D2::GFP-CASPL1D2* constructs were obtained using the In-Fusion® cloning technology (Clontech®) according to the manufacturer's instructions and checked by sequencing. First, to fuse cDNA sequences of *CASPL1D1* and *CASPL1D2* with *GFP*, *CASPL1D1* and *CASPL1D2* were cloned in pGWB5 and pGWB6 vectors, respectively, as described above for Gateway® cloning. *pCASPL1D1*, *CASPL1D1-GFP*, *pCASPL1D2* and *GFP-CASPL1D2* sequences were then amplified by PCR (iProof™ High-Fidelity PCR kit, Biorad) using the primers described in Table S2. *pCASPL1D1* and *CASPL1D1-GFP* sequences were also fused by PCR. *pCASPL1D1::CASPL1D1-GFP* sequence in one hand, and *pCASPL1D2*, *GFP-CASPL1D2* sequences in another hand, were introduced (In-Fusion®, Clontech®) into a pBSK vector containing RBCS terminator sequence and previously digested with the proper restriction enzymes [EcoRI/SacI (Fast Digest, ThermoScientific) and EcoRI/XbaI (Fast Digest, ThermoScientific) for *pCASPL1D1::CASPL1D1-GFP* and *pCASPL1D2::GFP-CASPL1D2*

constructs, respectively] according to manufacturer's instructions. *pCASPL1D1::CASPL1D1-GFP* and *pCASPL1D2::GFP-CASPL1D2* fused to RBCS terminator sequence were then digested with EcoRI/ClaI restriction enzymes (Fast Digest, ThermoScientific) and ligated into pGreen0179 (T4-DNA ligase, Promega) according to manufacturer's instructions.

2.2 - Plant materials and growth conditions

T-DNA insertion mutants were obtained from Bielefeld University [*caspl1b1.2* (Gabi-255B06), *caspl1d1.1* (Gabi-314C07)] and from the Nottingham *Arabidopsis* Stock Center [*caspl1b1.1* (Sail114-C02), *caspl1b2.1* (Salk-201916)] which also provided the transposon mutants [*caspl1d2.1* (SM-3-35485), *caspl1d2.2* (SM-3-28273)] (Figure S1). Plants were genotyped by PCR (Phire Plant Direct PCR kit, Thermo Scientific) using the primers listed in Table S3. Since *caspl1b1.1*, *caspl1b1.2*, *caspl1d1.1* and *caspl1d2.1* were obtained as heterozygous segregating seeds, plants homozygous for the absence of T-DNA insertion were isolated, renamed $WT_{b1.1}$, $WT_{b1.2}$, $WT_{d1.1}$ and WT_{d2}, respectively, and used further as control plants. Since *caspl1b2.1* and *caspl1d2.2* were provided as homozygous mutant lines, N60000 (Nottingham *Arabidopsis* Stock Center, renamed $WT_{b2.1}$) and WT_{d2} were used as controls for *caspl1b2.1* and *caspl1d2.2* plants, respectively. The *caspl1b1*caspl1b2* and *caspl1d1*caspl1d2* double mutant lines were obtained by crossing *caspl1b1.2* with *caspl1b2.1* and *caspl1d1.1* with *caspl1d2.1*, respectively. In the segregating seeds, 2 to 3 plants homozygous for both mutations (*caspl1b1*caspl1b2* and *caspl1d1*caspl1d2,* respectively*)* and 2 to 3 plants homozygous for the absence of the two mutations (WT_{b1*b2} and WT_{d1*d2}, respectively*)* were isolated and amplified. Analyses of the double mutant lines reported in this work consist of the combined phenotyping of these independent lines. *Promoter::GUS* and fusion proteins constructs were introduced into *Arabidopsis thaliana*

(ecotype Ws-2 and Col-0, respectively) plants *via Agrobacterium tumefaciens* GV3101 by the floral dip method (Clough & Bent, 1998) and transgenic lines were screened according to hygromycin (40 mg mL^{-1}) resistance (Harrison et al. 2006). *Arabidopsis* (Shahzad et al. 2016) and *Nicotiana tabacum* (Bellati et al. 2016) plants were grown as described previously.

2.3 - RNA isolation and RT–qPCR analysis

For each genotype, total RNA was extracted from 2 to 3 samples made of roots of 3 individual 3-week-old plants grown in hydroponics. RNA was extracted by a 5 min incubation at room temperature in 1 mL TRI reagent® (Sigma). To separate nucleic acids from proteins, samples were incubated for 5 min at room temperature in 200 µL of a 24:1 solution of chloroform/isoamyl alcohol (*v/v*) followed by a centrifugation at 20,000 *g* for 10 min. The RNA fraction was then treated with DNase (RQ1 RNase-Free DNase, Promega) and purified by two phenol/chloroform and one chloroform extractions. Reverse transcription (M-MLV Reverse Transcriptase, RNase H minus, Point Mutant; Promega) was performed with 1 µg of purified RNA using oligo$(dT)_{15}$ primer (Promega). Gene expression level was measured by RT-qPCR (LightCycler® LC480 II, Roche) using SYBR® Premix Ex Taq™ Tli RNaseH plus (Takara) and primers listed in Table S4. All real-time RT–PCR assays were conducted in triplicate for the same sample. Measurements were calibrated with a standard range composed of dilution series of a mix of all the samples and derived from Cp values calculated according to the second derivative maximum method (LightCycler® LC480 II, Roche). Expression data were normalized to expression of three housekeeping genes: *MON1* (At2g28390), *TIP41* (At4g34270) and *PP2AA3* (At1g13320). Data from mutant and control plants were compared using a two-tailed Student's *t* test.

2.4 - Root hydraulic conductivity and solute flow measurements

Root hydrostatic hydraulic conductivity ($Lp_{r\text{-}h}$) measurements were performed on 3-week-old plants grown in hydroponics, as described elsewhere (Shahzad et al. 2016). Root osmotic hydraulic conductivity ($Lp_{r\text{-}o}$) measurements were performed as described in (Postaire et al. 2010) with some modifications. No treatment with glucose was applied and the exuded sap flow (J_v, L hr^{-1}) was measured over the 45 min to 1 hr following hypocotyl excision. Solute flow through the root (J_s, mosm g^{-1} hr^{-1}) was calculated according to the formula $J_s=\Pi_s*J_v/(R*T*DW_r)$ where Π_s is the osmolality of the sap (mosm), R the gas constant, T the temperature (K) and DW_r the root dry weight (g).

2.5 - Functional expression in *Xenopus* oocytes

pGem-GWC plasmids containing the desired cDNA sequences were linearized by digestion with *Nhe*I (Thermo Scientific). Complementary RNA (cRNA) production, expression in *Xenopus laevis* oocytes and osmotic water permeability (P_f) measurements were performed as previously described (Maurel et al. 1993). For each independent biological repeat, P_f data were normalized to the mean P_f value of oocytes expressing the wild-type form of PIP2;1 and compared by one-way ANOVA followed by a Newman-Keuls test.

2.6 - GUS staining

Staining for GUS activity was performed as described previously (Postaire *et al.*, 2010) using 2 to 5 T1 generation plants from each of 3 to 4 independent lines grown *in vitro* for 7 to 8 days. To obtain cross sections, roots were embedded in Technovit® 7100 resin (Kulzer) according to the supplier instructions. The samples were pre-incubated for 2 hr in a 1:1 (*v/v)* solution of absolute ethanol/embedding solution (Technovit® 7100 + hardener 1) before

being incubated at 4 °C overnight in the embedding solution. The samples were then transferred to an inclusion solution (Technovit® 7100 + hardener 1 + hardener 2) for 1 hr at room temperature and for 3 days at 37°C. Five µm sections were performed with a Leica RM2165 microtome.

2.7 - Fluorol Yellow staining and suberization phenotyping

Five-day-old *in vitro* grown *Arabidopsis* plants were stained with Fluorol Yellow as previously described (Pfister et al. 2014). The observations were performed as described previously (Barberon et al. 2016) or with a Zeiss Observer 7 microscope with a 10X objective (EC Plan Neofluar, NA = 0.3, WD = 5.2 mm). In the latter case, excitation was done with a 470/40 nm filter and fluorescence emission was collected with a GFP filter (dichroic BS FT 495, emission window: 500 - 550 nm). For each root, fluorescent and bright field pictures were obtained to localize the starting point of the different suberization zones. The entire root was then imaged in transmitted light using the tiles and stiching modes of the Zen software. The percentage of length of the different zones (continuous suberization, discontinuous suberization, no suberization) according to the total root length was calculated using an ImageJ software.

2.8 - Confocal imaging

Confocal imaging were performed with 5-day-old *in vitro* grown *Arabidopsis* plants using a Leica TCS SP8 laser scanning microscope with a 40X water N.A. 1,3 immersion objective. GFP and FM4-64/propidium iodide were excited at 488 and 561 nm, respectively, and emission fluorescence was collected in line sequential scanning mode between 500 and 540 nm, 600 and 650 nm and 630 and 700 nm for GFP, propidium iodide and FM4-64, respectively.

2.9 - Fluorescence Lifetime Imaging

FLIM experiments were conducted according to (Bellati et al. 2016) except that the measurements were performed 2 days after infiltration of tobacco (*N. tabacum* cv SR1) plants with *Agrobacterium tumefaciens* GV3101 solution exhibiting an optical density of 0.01 at 600 nm for GFP constructs and 0.005 for RFP constructs and that GFP was excited for 2 min.

2.10 - Immuno-purification and mass spectrometry analysis

See supplemental methods

3 - RESULTS

3.1 - Expression patterns of *CASPLs* genes in roots and subcellular localization of corresponding proteins

Although expression of *CASPL1D2* has been reported in endodermis and cells overlaying the basis of lateral roots (Roppolo et al. 2014), little information is available regarding the expression pattern of other *CASPLs* (Roppolo et al. 2014). To get further insights into expression of the four *CASPLs* of interest, upstream regulatory sequences were fused translationally to the *β-glucuronidase* (*GUS*) gene and transferred into *Arabidopsis.* Promoter sequences (*pCASPL1B1*, *pCASPL1B2s*, *pCASPL1D1*, *pCASPL1D2*) were defined as the genomic DNA sequence upstream of the starting codon of the gene of interest, up to the end of the open reading frame of the neighboring gene. Because in the case of *CASPL1B2*, such a defined sequence (*pCASPL1B2s*) is rather short (629 bp), another promoter fragment (*pCASPL1B2l*) corresponding to the 2kb genomic DNA sequence upstream of *CASPL1B2* was also investigated. Since GUS activity patterns were similar in lines expressing

pCASPL1B2s::GUS and *pCASPL1B2l::GUS* (data not shown), the text further refers indistinctly to these two constructs as *pCASPL1B2::GUS*.

Roots of seedlings expressing the *pCASPL1B1::GUS*, *pCASPL1B2*::*GUS* or *pCASPL1D2::GUS* constructs revealed very similar expression patterns. In these lines, no GUS activity was observed in root tips and youngest tissues (Figure 1a); in contrast, GUS activity was observed in the endodermis, first with a patchy pattern (Figures 1b,c, Figures S2b,c) then continuously (Figures 1d,e, Figures S2d,e) in oldest root segments. In addition, no staining was observed in some endodermis cells facing xylem poles (Figure 1f), suggesting that *CASPL1B1*, *CASPL1B2* and *CASPL1D2* may not be expressed in passage cells. Finally, GUS activity was also observed in cells overlaying the basis of lateral roots (Figure 1g, Figures S2f,g). By contrast to the other lines, lines expressing the *pCASPL1D1::GUS* construct showed some GUS activity in root tips (Figure 1h) and in younger tissues (Figures 1a,i,j). In these plants, GUS activity was observed in every cell type of the root (Figures 1i,j) suggesting that *CASPL1D1* has a broader root expression pattern than the 3 other *CASPL* genes.

To determine the expression patterns of the corresponding proteins, we investigated transgenic *Arabidopsis* plants expressing fusion proteins under their endogenous *CASPL* promoter. Regarding CASPLB proteins, we failed to obtain corresponding transgenic lines. In contrast, 5-day-old transgenic plants expressing *pCASPL1D1::CASPL1D1-GFP* or *pCASPL1D2::GFP-CASPL1D2* revealed that CASPL1D1 was mostly expressed in the cortex close to the root tip and in a continuous way along the root (Figure S3A, C) while CASPL1D2 was not expressed in younger tissues but expressed later in the endodermis in a discontinuous (within about 29 % of mid root length) then continuous way (within about 29 % of basal root length) (Figure S3B, C). These observations confirm the GUS expression data and point to a specific expression of CASPL1D1 in the cortex.

Previous work by (Roppolo et al. 2014) showed that, when expressed under a *CASP1* promoter, CASPL1B2, CASPL1D1 and CASPL1D2 localize to the plasma membrane (Roppolo et al. 2014). Whereas CASPL1B2 was enriched in the CSD, CASPL1D1 and CASPL1D2 were excluded from this domain (Roppolo et al. 2014). In the present study, we confirmed the plasma membrane localization of CASPL1D1 and CASPL1D2 in cortex and endodermis, respectively (Figure S4) together with the exclusion of CASPL1D2 from the CSD (Figure S5). Since PIP2;1 is expressed in the plasma membrane of almost every root cell type (Peret et al., 2012), the 4 CASPLs studied in this work are potentially co-expressed with the aquaporin. In particular, 3 of these CASPLs may co-localize with PIP2;1 at the plasma membrane of cortical cells (CASPL1D1) or endodermal cells (CASPL1B2 and CASPL1D2) allowing a putative functional interaction with the aquaporin.

3.2 - Suberization of plants with altered *CASPL* expression

The expression of *CASPL1B1, CASPL1B2* and *CASPL1D2* in the endodermis, with a patchy and thereafter continuous pattern (Figure 1), their lack of expression in passage cells but expression in cells overlaying the basis of lateral roots (Figure 1) match the pattern of root suberization (Andersen et al. 2018; Naseer et al. 2012). These observations suggest that these genes could be involved in this process rather than in Casparian strip formation taking place in younger endodermal cells. To address this point, we isolated T-DNA or transposon insertion lines for each gene (*caspl1b1.1*, *caspl1b1.2*, *caspl1b2.1*, *caspl1d1.1*, *caspl1d2.1, caspl1d2.2*) (Figure S1). To circumvent putative functional redundancies, we also generated double mutant lines (*caspl1b1*caspl1b2* and *caspl1d1*caspl1d2*) by crossing single mutant lines of the closest homologs. RT-qPCR analysis of plants cultivated in hydroponics revealed a dramatic reduction (>89%) of *CASPL1B1*, *CASPL1B2* and *CASPL1D2* expression in the

corresponding mutant lines and, compared to their respective control lines, a 73% and 76% decrease of *CASPL1D1* expression in *caspl1d1.1* and *caspl1d1*caspl1d2*, respectively (Figure S6). Moreover, no difference in root and shoot dry weights (Table S5) was observed between the single and double *caspl* mutant plants and their respective controls.

*caspl1b1*caspl1b2* and *caspl1d1*caspl1d2* double mutant lines and their respective control lines (WT_{b1*b2} and WT_{d1*d2}) were whole mount stained with Fluorol Yellow, a suberin fluorescent dye (Naseer et al. 2012). In initial experiments (Figure 2), roots of both control and double mutant plants were continuously suberized along 29.5% (for *caspl1d1*caspl1d2*) to 38% (for *caspl1b1*caspl1b2*) of their length and showed a patchy suberization pattern on 25% (for *caspl1b1*caspl1b2*) to 30.5% of their length (for *caspl1d1*caspl1d2*) (Figure 2). However, no significant difference could be measured between the double mutant lines and their respective controls (Figure 2) suggesting that, under these standard growth conditions, neither CASPL1B1 and CASPL1B2 nor CASPL1D1 and CASPL1D2 significantly interfere with the endodermis suberization pattern.

As a transcellular barrier, suberin can also interfere with root nutrient uptake (Barberon et al. 2016; Li et al. 2017). Thus, the 4 CASPLs could act more significantly on the barrier permeability than on the whole deposition of suberin *per se*. This hypothesis was tested by examining solute flows (J_s) deduced from root exudation measurements. No significant difference in J_s was measured between *caspl* single or double mutant plants and their respective control plants (Figure S7). These results indicate that the 4 CASPLs do not have a major effect on total solute uptake by the root and on the permeability of the suberin barrier.

The *MYB41* (At4g28110) transcription factor of *Arabidopsis* was recently shown to promote the expression of suberin biosynthesis genes (Kosma et al. 2014). While *MYB41*

shows no expression in roots under standard culture conditions, its expression is induced in the endodermis in response to ABA and NaCl (Kosma et al. 2014), two stimuli known to induce an over-suberization of the endodermis (Barberon et al. 2016). Interestingly, *CASPL1D2* is the most highly upregulated gene (showing a 300-fold induction) in transgenic plants over-expressing *MYB41*. In contrast, expression of *CASPL1B1* and *CASPL1B2* remains unchanged (Cominelli et al. 2008). To test a putative role of CASPL1D2 and its closest homolog, CASPL1D1, in endodermis over-suberization in response to ABA and NaCl stress, the *caspl1d1*caspl1d2* double mutant line and its control line (WT_{d1*d2}) were treated with 1 µM ABA or 100 mM NaCl for 6 hr prior to Fluorol Yellow staining (Figure 3). In control conditions, and by contrast to previous observations (Figure 2), *caspl1d1*caspl1d2* exhibited a slightly but significantly longer continuous suberization zone (42% of endodermal cells) than WT_{d1*d2} (36% of endodermal cells) (Figure 3a, b), suggesting that endodermis suberization may be negatively affected by CASPL1D1 and CASPL1D2. Upon a 6 hour-ABA treatment, the continuous suberization zone increased and represented 58% of endodermal cells in the two genotypes (Figure 3a). Increasing the treatment duration to 14 hr resulted in a stronger enhanced suberization with a continuous suberization zone representing 81 % of endodermal cells in both WT_{d1*d2} and *caspl1d1*caspl1d2* (Figure S8). These results suggest that, in the control conditions of some experiments, CASPL1D1 and CASPL1D2 can act as negative regulators of endodermis suberization and, by contrast, in the presence of ABA, additional molecular events would compensate the initial difference between the two genotypes.

In the two genotypes, salt treatment induced an over deposition of suberin illustrated by a longer continuous suberization zone: 50% and 56% of endodermal cells in this zone are suberized in WT_{d1*d2} and *caspl1d1*caspl1d2*, respectively (Figure 3b, Figure S9). Such a

higher suberization in *caspl1d1*caspl1d2* is consistent with the phenotype of this line under control conditions. However, the data do not reveal any specific role of CASPL1D1 and CASPL1D2 in suberin over-deposition upon a salt treatment.

In summary, endodermis suberization may be affected by CASPL1D1 and CASPL1D2 in control and NaCl conditions but not in the presence of ABA.

3.3 - Root water transport in plants with altered *CASPL* expression

The 4 CASPLs co-purify with GFP-PIP2;1 in a total root protein extract of *35S::GFP-PIP2;1* plants (Bellati et al. 2016). In addition, *PIP2;1* is expressed in the endodermis (Peret et al. 2012), similar to the four CASPLs (see above). Thus, the latter could act as regulators of PIP2;1 and more generally of aquaporins *in planta*.

Aquaporins contribute to about 70% of Lp_r in *Arabidopsis* [(Maurel et al. 2015), for review]. Here, we used two different techniques to characterize root water transport in *caspl* mutant plants. The pressure chamber technique (Boursiac et al. 2005), which somehow mimics the force exerted onto the root during transpiration, was used to characterize the root hydrostatic hydraulic conductivity ($Lp_{r\text{-}h}$). Spontaneous exudation, which is driven by nutrient uptake and mimics root pressure, the main driving force of water flow during the night, was used to deduce the root osmotic permeability ($Lp_{r\text{-}o}$) (Postaire et al. 2010). Neither the single mutants (*caspl1b1.1*, *caspl1b1.2*, *caspl1b2.1, caspl1d1.1, caspl1d2.1* and *caspl1d2.2*) nor the double mutants (*caspl1b1*caspl1b2* and *caspl1d1*caspl1d2*) showed any significant alteration in $Lp_{r\text{-}h}$ compared to their respective control lines (Figure 4a). A tendency to a decreased $Lp_{r\text{-}o}$ was observed for *caspl1d2.1* and *caspl1d2.2* lines but was not confirmed in the *caspl1d1*caspl1d2* double mutant. Overall, no significant difference in $Lp_{r\text{-}o}$ was measured between *caspl* single or double mutant lines and

their respective controls (Figure 4b). Thus, loss-of-function of *CASPL* genes does not affect root water transport in our experimental conditions.

Root water transport is contributed by the symplastic, transcellular and the apoplastic pathways. A putative compensation between these pathways may impair the detection of a root hydraulic phenotype in *caspl* plants. In order to distinguish between the contribution to $Lp_{r\text{-}h}$ of aquaporin-dependent (*i.e.* transcellular) and aquaporin-independent pathways, *caspl* and control plants were treated with 1 mM sodium azide, a reversible aquaporin blocker (Tournaire-Roux et al. 2003). Except for one allele of *caspl1b1* (*caspl1b1.1*) which exhibited a 25% decrease in the aquaporin-independent $Lp_{r\text{-}h}$, none of the *caspl* mutants displayed significant phenotypical differences with regard to the control genotypes (Figure 4a). These results indicate that CASPLs do not act on the aquaporin-dependent or -independent water transport pathways in roots under control conditions. With regard to the *MYB41* induction in response to ABA and salt (Kosma et al. 2014) and to the up-regulation of *CASPL1D2* in transgenic plants over-expressing *MYB41* (Cominelli et al. 2008), ABA and NaCl, two treatments also described to decrease aquaporin function and thus Lp_r (Boursiac et al., 2005, Aroca et al., 2003) were compared in WT_{d1*d2} and *caspl1d1*caspl1d2* plants. A treatment of WT_{d1*d2} and *caspl1d1*caspl1d2* plants with 1 µM ABA for 6 hr decreased $Lp_{r\text{-}h}$ to the same extend in both genotypes (53 % and 49 % decrease, respectively) (Figure 5a). After a 6-hour-treatment with 100 mM NaCl, a tendency to a higher $Lp_{r\text{-}h}$ inhibition was observed in *caspl1d1*caspl1d2* (70% inhibition) compared to WT_{d1*d2} (52%) (Figure 5b).

3.4 - Functional interaction between PIP2;1 and CASPL1B1 and CASPL1D2

In view of the complexity of root systems, we next investigated a putative effect of CASPLs on aquaporins at the molecular level. CASPL1B1 and CASPL1D2 were selected for further

analysis, as representatives of the CASPL1B and CASPL1D subgroups, respectively. First, the interaction between CASPL1B1 or CASPL1D2 and PIP2;1 was characterized by FRET-FLIM after transient expression in tobacco leaf epidermal cells of the two putative interacting partners tagged with GFP and RFP, respectively. The guanine nucleotide-binding protein AGG1 (At3g63420), a prenylated protein anchored to the plasma membrane, was used as a negative control for physical interactions with CASPL1B1 and CASPL1D2. Indeed no significant decrease in GFP-CASPL1B1 or CASPL1D2-GFP fluorescence lifetime was observed in the presence of RFP-AGG1. In the presence of RFP-PIP2;1, however, a significant (p<0.05) decrease in GFP fluorescence lifetime was measured for both GFP-CASPL1B1 and CASPL1D2-GFP (Table 1) indicating that both CASPL1B1 and CASPL1D2 physically interact with PIP2;1 (Table 1). Next, expression in *Xenopus laevis* oocytes was used to investigate a putative role of the two proteins in regulating PIP2;1 function. Expression of PIP2;1 alone conferred, with respect to native oocytes, a 8-fold increase in cell osmotic water permeability (P_f) (Figure 6a). Co-expression of PIP2;1 with 2 different quantities of CASPL1B1 (ratios of CASPL1B1/PIP2;1 cRNA molecules of 0.73 and 2.18) resulted in a further 25% increase in P_f (Figure 6a) indicating that CASPL1B1 can stimulate water transport by the aquaporin and that CASPL1B1 quantity does not seem to be a limiting factor. Although CASPL1D2 also physically interacts with PIP2;1, it failed to stimulate its water transport activity (Figure 6b).

Phosphorylation is an important molecular mechanism for regulation of PIPs, acting on both channel gating and protein subcellular trafficking [(Maurel et al. 2015), for review]. Phosphorylation can also interfere with protein-protein interactions (Betts et al. 2017). Four phosphorylation sites have been described in PIP2;1, at Ser121 (loop *B*), Ser277, Ser280 and Ser283 (C-terminal end) (Di Pietro et al. 2013, Grondin et al. 2015, Prak et al. 2008). In order to investigate the effect of the C-terminal tail phosphorylation of PIP2;1 on its interactions

with proteins, interactomes of PIP2;1 forms with Ser-to-Ala mutations (PIP2;1-AA) or Ser-to-Asp mutations (PIP2;1-DD) at positions 280 and 283 were compared using an immuno-purification (IP) strategy coupled to protein identification and quantification by mass spectrometry according to (Bellati et al. 2016) (Tables S6-S10). This analysis revealed that 55 and 142 proteins were specific for or specifically enriched in PIP2;1-AA and PIP2;1-DD interactome, respectively (Table S10). Thus, interactions of several proteins with PIP2;1 seem to partly depend on the level of its C-terminal phosphorylation. Interestingly, the abundance of CASPL1B1 was significantly increased by 1.4 in the interactome of PIP2;1-DD when compared to that of PIP2;1-AA (Tables S7, S10) suggesting that CASPL1B1 may preferentially interact with phosphorylated PIP2;1. We thus checked whether C-terminal phosphorylation of PIP2;1 could interfere with the aquaporin stimulation by CASPL1B1. Co-expression of CASPL1B1 with PIP2;1-DD, but not with PIP2;1-AA, increased the oocyte P_f by 25%, (Figure 7) indicating that CASPL1B1 specifically activates the aquaporin in its phosphorylated form. We then wondered whether the C-terminal phosphorylation of PIP2;1 was required for physical interaction between CASPL1B1 and PIP2;1, thereby explaining why PIP2;1-DD but not PIP2;1-AA showed functional activation with CASPL1B1. Physical interaction of CASPL1B1 with PIP2;1-DD and PIP2;1-AA was tested by FRET-FLIM measurements in tobacco leaf epidermal cells. A significant decrease in GFP-CASPL1B1 fluorescence lifetime was measured in presence of both RFP-PIP2;1-DD and RFP-PIP2;1-AA (Table 1) suggesting, at variance with the IP experiments, that physical interaction between CASPL1B1 and the aquaporin is not dependent on its phosphorylation. It is also deduced that stimulation of PIP2;1 by CASPL1B1 would involve two distinct and sequential processes: a physical interaction between the two partners and an activation of the aquaporin water

transport by CASPL1B1. Of these two processes, only the second one is dependent on C-terminal phosphorylation of the aquaporin.

4 - DISCUSSION

CASPL1B1, CASPL1B2, CASPL1D1 and CASPL1D2, four homologs of CASPs with unknown function have previously been identified as PIP2;1 interactants (Bellati et al. 2016). Our objectives here were to evaluate their role in cell wall modifications and regulation of root water transport and/or aquaporin function.

By homology with CASPs, CASPLs were first supposed to recruit proteins and enzymes involved in cell wall modifications (Roppolo et al. 2014). Interestingly, we observed that *CASPL1B1*, *CASPL1B2* and *CASPL1D2* show a spatio-temporal expression pattern that matches suberized territories (Figure 1). The combined disruption of close CASPL homologs, *CASPL1D1* and *CASPL1D2* (but not *CASPL1B1* and *CASPL1DB2*), was found to sometimes increase the root suberin deposition pattern in control conditions suggesting a surprising negative role of CASPL1D1 and CASPL1D2 in the continuous suberization of the root (Figure 3). Since this phenotype was not systematically observed (Figure 2, 3), we emphasize that the role of CASPL1D1 and CASPL1D2 in preventing continuous suberization in control conditions remains weak. We also noticed that over-expression of the *MYB41* (At4g28110) transcription factor in *Arabidopsis* can activate genes contributing to suberin synthesis (Kosma et al. 2014) in particular in response to ABA and NaCl (Kosma et al. 2014). Interestingly, *CASPL1D2* was reported as the most highly upregulated gene in transgenic plants over-expressing *MYB41*, whereas expression of *CASPL1B1* and *CASPL1B2* remained unchanged (Cominelli et al. 2008). However, no major difference in suberization pattern was observed between the WT_{d1*d2} control and the double mutant *caspl1d1*caspl1d2* in

response to both ABA and NaCl (Figure 3). Thus, the CASPL1D2 and CASPL1D1 homologs do not exert major effects on stress induced over-suberization of the root. In agreement with the reduced effects of CASPLs on root suberization, we failed to reveal defects in solute and aquaporin-independent water transport in roots of corresponding mutant plants, whether under control or stress conditions.

PIPs show a high degree of regulation through post-translational modifications and interactions with proteins such as modifying enzymes or proteins involved in vesicle trafficking. The present study pinpoints a novel regulatory mechanism of PIP2;1 involving CASPLs. These proteins are lowly expressed and barely detected in proteomic studies. Yet, 4 CASPLs were previously found to be enriched in a PIP interactome (Bellati et al. 2016) suggesting a functional interaction with aquaporins. Here, we show that CASPL1B1 stimulates PIP2;1 when expressed in *Xenopus* oocytes (Figure 6). Their physical interaction (Table 1) suggests a direct effect of CASPL1B1 on aquaporin gating, subcellular localization and/or stability. However, by analogy with CASPs which are responsible for the structuration of a membrane domain, the CSD [(Doblas et al. 2017), for review], CASPL1B1 function could also be linked to membrane domains regulating PIP2;1. PIPs have indeed been localized in microdomains of the plasma membrane (Minami et al. 2009; Mongrand et al. 2004, Morel et al. 2006). In *Arabidopsis* roots under NaCl stress, the enrichment of PIP2;1 in these microdomains was proposed to favor its internalization (Li et al. 2011). In the present case, the membrane domain scaffolded by CASPL1B1 would rather stimulate PIP2;1 activity. This could happen through recruitment of activating protein kinases, with functional homologs being present in native *Xenopus* oocytes. We note that the presence of such endogenous protein kinases is supported by negative effects of protein kinases inhibitors on activity of plant aquaporins in these cells (Amezcua-Romero et al. 2010, Azad at al. 2008, Johansson et

al. 1998, Van Wilder et al. 2008). Further, we suppose that, despite its physical interaction with PIP2;1 (Table 1), CASPL1D2 had no functional effect in oocytes (Figure 6), because of the lack of a critical protein partner(s) leading to PIP2;1 regulation. The regulation of PIP2;1 by CASPL1B1 seems to rely on a complex and highly regulated mechanism as it also depends on the phosphorylation status of the aquaporin. By combining 3D structures with phosphorylation data, it was recently demonstrated that phosphorylation can strengthen or weaken molecular connections, thereby contributing to regulation of numerous biological processes (Betts et al. 2017). Interactomics using IP methodology can reveal direct and indirect protein-protein interactions. Such an analysis, indicating a 1.4-fold enrichment of CASPL1B1 in the PIP2;1-DD interactome as compared to PIP2;1-AA interactome (Table S7), suggested that CASPL1B1 preferentially interacts with PIP2;1 in its phosphorylated form. This result may appear at variance with FRET-FLIM data showing that CASPL1B1 directly interacts with PIP2;1, independent of its C-terminal phosphorylation status (Table 1). In our conditions, however, FLIM may not have been sensitive enough to assess the slight preference in interaction revealed by IP. Furthermore, differences in position of the fluorophore in the fusion proteins (*i.e.* at the N-terminus and C-terminus, in IP and FLIM experiments, respectively) and differences in the biological systems used (*i.e. Arabidopsis* root cells and tobacco leaf epidermal cells in IP and FLIM experiments, respectively), may also contribute to explain such a discrepancy. Despite these uncertainties about the role of phosphorylation in PIP2;1 - CASPL1B1 interactions, our data revealed a clear role of aquaporin phosphorylation in aquaporin activation by CASPL1B1. In the plant, CASPL1B1 is much less abundant than PIP2;1. Thus, when co-expressing PIP2;1-AA and CASPL1B1 in *Xenopus* oocytes, with a CASPL1B1/PIP2;1 cRNA molecular ratio of 2.18, we somehow forced the interaction between the two partners. Despite this, CASPL1B1 was not able to

activate PIP2;1-AA (Figure 7). Thus, the direct interaction between CASPL1B1 and PIP2;1 is not sufficient to activate PIP2;1 but requires complementary aquaporin phosphorylation.

PIPs share a high degree of sequence homology (more than 75%) and many isoforms are expressed in the endodermis (Javot et al. 2003; Peret et al. 2012, Petricka et al. 2012, Postaire et al. 2010). The identification of CASPL1B1 in the interactome of both PIP2;1 and PIP1;2 (Bellati et al. 2016) further suggests that CASPL1B1 may interact with and stimulate multiple PIPs *in planta*. Considering that aquaporins largely contribute to Lp_r in *Arabidopsis* [(Maurel et al. 2015), for review], it may be surprising that we failed in revealing a Lp_r phenotype in *caspl1b1* and c*aspl1b1*caspl1b2* mutants (Figure 4). We note however that *CASPL1B1* expression is restricted to suberized cells (Figure 1) and that the contribution of these cells to overall root water flow may actually be low and not measurable. Indeed, suberin lamellas are barriers limiting the transcellular diffusion of water and ions through the endodermal cell plasma-membrane (Bellati et al. 2016). Thus, aquaporins present in this membrane may rather control the osmolality of these cells.

In conclusion, the CASPLs are likely to have different functional roles in the endodermis and the present work identifies a novel type of potential regulation of PIP2;1 by a protein from the CASPL family. At the molecular level, we show that the activation process of aquaporin PIP2;1 by CASPL1B1 requires a direct interaction between the two partners and an additional aquaporin phosphorylation involving a putative third partner. In addition, the CASPL1Ds roles may be associated with suberization under with abiotic stress.

ACKNOWLEDGMENTS

We thank Xavier Dumont and Philippe Rieu for their contribution to plant transformation and suberization studies, respectively, Linnka Lefebvre-Legendre for technical help and the

Mass Spectrometry Proteomics Platform (MSPP) for its technical support in proteomics experiments. FLIM measurements were performed on MRI (Montpellier Rio Imaging platform, Montpellier), and the technical help of Carine Alcon, Sylvain Rossi and Alexandre Martinière is fully acknowledged.

REFERENCES

Amezcua-Romero J.C., Pantoja O. & Vera-Estrella R. (2010) Ser123 is essential for the water channel activity of McPIP2;1 from *Mesembryanthemum crystallinum*. *Journal of Biological Chemistry*, **285**, 16739-16747.

Andersen T.G., Naseer S., Ursache R., Wybouw B., Smet W., De Rybel B., Vermeer J.E.M. & Geldner N. (2018) Diffusible repression of cytokinin signalling produces endodermal symmetry and passage cells. *Nature*, **555**, 529-533

Azad A.K., Katsuhara M., Sawa Y., Ishikawa T. & Shibata H. (2008) Characterization of four plasma membrane aquaporins in tulip petals: A putative homolog is regulated by phosphorylation. *Plant Cell Physiol.*, **49**, 1196-1208.

Barberon M., Vermeer J.E.M., De Bellis D., Wang P., Naseer S., Andersen T.G., …, Geldner N. (2016) Adaptation of Root Function by Nutrient-Induced Plasticity of Endodermal Differentiation. *Cell*, **164**, 447-459.

Bellati J., Champeyroux C., Hem S., Rofidal V., Krouk G., Maurel C. & Santoni V. (2016) Novel aquaporin regulatory mechanisms revealed by interactomics. *Molecular and Cellular Proteomics*, **15**, 3473-3487.

Besserer A., Burnotte E., Bienert G.P., Chevalier A.S., Errachid A., Grefen C., …, Chaumont F. (2012) Selective Regulation of Maize Plasma Membrane Aquaporin Trafficking and Activity by the SNARE SYP121. *Plant Cell*, **24**, 3463-3481.

Betts M.J., Wichmann O., Utz M., Andre T., Petsalaki E., Minguez P., …, Russell R.B. (2017) Systematic identification of phosphorylation-mediated protein interaction switches. *Plos Computational Biology*, **13**.

Boursiac Y., Chen S., Luu D.-T., Sorieul M., van den Dries N. & Maurel C. (2005) Early effects of salinity on water transport in *Arabidopsis* roots. Molecular and cellular features of aquaporin expression. *Plant Physiology*, **139**, 790-805.

Chen W., Yin X., Wang L., Tian J., Yang R.Y., Liu D.F., …, Gao J.P. (2013) Involvement of rose aquaporin *Rh*PIP1;1 in ethylene-regulated petal expansion through interaction with *Rh*PIP2;1. *Plant Molecular Biology*, **83**, 219-233.

Clough S.J. & Bent A.F. (1998) Floral dip: a simplified method for *Agrobacterium*-mediated transformation of *Arabidopsis thaliana*. *Plant Journal*, **16**, 735-743.

Cominelli E., Sala T., Calvi D., Gusmaroli G. & Tonelli C. (2008) Over-expression of the Arabidopsis AtMYB41 gene alters cell expansion and leaf surface permeability. *Plant Journal*, **53**, 53-64.

Di Pietro M., Vialaret J., Li G.-W., Hem S., Prado K., Rossignol M., …, Santoni V. (2013) Coordinated post-translational responses of aquaporins to abiotic and nutritional stimuli in *Arabidopsis* roots. *Molecular and Cellular Proteomics*, **12**, 3886-3897.

Doblas V.G., Geldner N. & Barberon M. (2017) The endodermis, a tightly controlled barrier for nutrients. *Current Opinion in Plant Biology*, **39**, 136-143.

Geldner N. (2013) Casparian strips. *Current Biology*, **23**, R1025-R1026.

Grondin A., Rodrigues O., Verdoucq L., Merlot S., Leonhardt N. & Maurel C. (2015) Aquaporins contribute to ABA-triggered stomatal closure through OST1-mediated phosphorylation. *Plant Cell*, **27**, 1-11.

Hachez C., Laloux T., Reinhardt H., Cavez D., Degand H., Grefen C., …, Chaumont F. (2014) Arabidopsis SNAREs SYP61 and SYP121 coordinate the trafficking of plasma membrane aquaporin PIP2;7 to modulate the cell membrane water permeability. *Plant Cell*, **26**, 3132-3147.

Hachez C., Veljanovski V., Reinhardt H., Guillaumot D., Vanhee C., Chaumont F. & Batoko H. (2014) The Arabidopsis abiotic stress-induced TSPO-related protein reduces cell-surface expression of the aquaporin PIP2;7 through protein-protein interactions and autophagic degradation. *Plant Cell*, **26**, 4974-4990.

Harrison S.J., Mott E.K., Parsley K., Aspinall S., Gray J.C. & Cottage A. (2006) A rapid and robust method of identifying transformed Arabidopsis thaliana seedlings following floral dip transformation. *Plant Methods*, **2**.

Javot H., Lauvergeat V., Santoni V., Martin F., Güclü J., Vinh J., …, Maurel C. (2003) Role for a single aquaporin isoform in root water uptake. *Plant Cell*, **15**, 509-522.

Johanson U. & Gustavsson S. (2002) A new subfamily of major intrinsic proteins in plants. *Molecular Biology and Evolution* **19**, 456-461.

Johansson I., Karlsson M., Shukla V.K., Chrispeels M.J., Larsson C. & Kjellbom P. (1998) Water transport activity of the plasma membrane aquaporin PM28A is regulated by phosphorylation. *Plant Cell*, **10**, 451-459.

Kaldenhoff R., Ribas-Carbo M., Flexas J., Lovisolo C., Heckwolf M. & Uehlein N. (2008) Aquaporins and plant water balance. *Plant Cell and Environment*, **31**, 658-666.

Karimi M., Inze D. & Depicker A. (2002) GATEWAY((TM)) vectors for Agrobacterium-mediated plant transformation. *Trends in Plant Science*, **7**, 193-195.

Kosma D.K., Murmu J., Razeq F.M., Santos P., Bourgault R., Molina I. & Rowland O. (2014) AtMYB41 activates ectopic suberin synthesis and assembly in multiple plant species and cell types. *Plant Journal*, **80**, 216-229.

Lee H.K., Cho S.K., Son O., Xu Z., Hwang I. & Kim W.T. (2009) Drought stress-induced Rma1H1, a RING membrane-anchor E3 ubiquitin ligase homolog, regulates aquaporin levels via ubiquitination in transgenic *Arabidopsis* plants. *Plant Cell*, **21**, 622-641.

Li B.H., Kamiya T., Kalmbach L., Yamagami M., Yamaguchi K., Shigenobu S., …, Fujiwara T. (2017) Role of LOTR1 in Nutrient Transport through Organization of Spatial Distribution of Root Endodermal Barriers. *Current Biology*, **27**, 758-765.

Li D.D., Ruan X.M., Zhang J., Wu Y.J., Wang X.L. & Li X.B. (2013) Cotton plasma membrane intrinsic protein 2s (PIP2s) selectively interact to regulate their water channel activities and are required for fibre development. *New Phytologist*, **199**, 695-707.

Li L., Wang H., Gago J., Cui H.Y., Qian Z.J., Kodama N., Ji H.T., …, Dong H.S. (2015) Harpin Hpa1 Interacts with Aquaporin PIP1;4 to Promote the Substrate Transport and Photosynthesis in Arabidopsis. *Scientific Reports*, **5**.

Li X.J., Wang X.H., Yang Y., Li R.L., He Q.H., Fang X.H., …, Lin J.X. (2011) Single-molecule analysis of PIP2;1 dynamics and partitioning reveals multiple modes of *Arabidopsis* plasma membrane aquaporin regulation. *Plant Cell*, **23**, 3780-3797.

Liman E.R., Tytgat J. & Hess P. (1992) Subunit stoichiometry of a mamalian K^+ channel determined by construction of multimeric cDNAs. *Neuron*, **9**, 861-871.

Martiniere A., Lavagi I., Nageswaran G., Rolfe D.J., Maneta-Peyret L., Luu D.T., …, Runions J. (2012) Cell wall constrains lateral diffusion of plant plasma-membrane proteins. *Proceedings of the National Academy of Sciences of the United States of America*, **109**, 12805-12810.

Maurel C., Boursiac Y., Luu D.-T., Santoni V., Shahzad Z. & Verdoucq L. (2015) Aquaporins in Plants. *Physiological reviews*, **95**, 1321-1358.

Maurel C., Reizer J., Schroeder J.I. & Chrispeels M.J. (1993) The vacuolar membrane protein γ-TIP creates water specific channels in *Xenopus* oocytes. *EMBO Journal*, **12**, 2241-2247.

Maurel C., Verdoucq L., Luu D.-T. & Santoni V. (2008) Plant aquaporins: membrane channels with multiple integrated functions. *Annual Review of Plant Biology*, **59**, 595-624.

Minami A., Fujiwara M., Furuto A., Fukao Y., Yamashita T., Kamo M., Kawamura Y. & Uemura M. (2009) Alterations in detergent-resistant plasma membrane microdomains in *Arabidopsis thaliana* during cold acclimation. *Plant Cell Physiology*, **50**, 341-359.

Mongrand S., Morel J., Laroche J., Claverol S., Carde J.P., Hartmann M.A., Bonneu M., Simon-Plas F., Lessire R. & Bessoule J.J. (2004) Lipid rafts in higher plant cells: purification and characterization of Triton X-100-insoluble microdomains from tobacco plasma membrane. *Journal of Biological Chemistry*, **279**, 36277-36286.

Morel J., Claverol S., Mongrand S., Furt F., Fromentin J., Bessoule J.J., Blein J.P. & Simon-Plas F. (2006) Proteomics of plant detergent-resistant membranes. *Molecular and Cellular Proteomics*, **5**, 1396-1411.

Nakagawa T., Suzuki T., Murata S., Nakamura S., Hino T., Maeo K., …, Ishiguro S. (2007) Improved gateway binary vectors: High-performance vectors for creation of fusion constructs in Transgenic analysis of plants. *Bioscience Biotechnology and Biochemistry*, **71**, 2095-2100.

Naseer S., Lee Y., Lapierre C., Franke R., Nawrath C. & Geldner N. (2012) Casparian strip diffusion barrier in Arabidopsis is made of a lignin polymer without suberin. *Proceedings of the National Academy of Sciences of the United States of America*, **109**, 10101-10106.

Peret B., Li G.W., Zhao J., Band L.R., Voss U., Postaire O., …, Bennett M.J. (2012) Auxin regulates aquaporin function to facilitate lateral root emergence. *Nature Cell Biology*, **14**, 991-998.

Petricka J.J., Schauer M.A., Megraw M., Breakfield N.W., Thompson J.W., Georgiev S., …, Benfey P.N. (2012) The protein expression landscape of the Arabidopsis root. *Proceedings of the National Academy of Sciences of the United States of America*, **109**, 6811-6818.

Pfister A., Barberon M., Alassimone J., Kalmbach L., Lee Y., Vermeer J.E.M., …, Geldner N. (2014) A receptor-like kinase mutant with absent endodermal diffusion barrier displays selective nutrient homeostasis defects. *Elife*, **3**.

Postaire O., Tournaire-Roux C., Grondin A., Boursiac Y., Morillon R., Schäffner T. & Maurel C. (2010) A PIP1 aquaporin contributes to hydrostatic pressure-induced water transport in both the root and rosette of *Arabidopsis*. *Plant Physiology*, **152**, 1418-1430.

Prak S., Hem S., Boudet J., Viennois J., Sommerer N., Rossignol R., …, Santoni V. (2008) Multiple phosphorylations in the C-terminal tail of plant plasma membrane aquaporins. Role in sub-

cellular trafficking of *At*PIP2;1 in response to salt stress *Molecular and Cellular Proteomics*, **7**, 1019-1030.

Quigley F., Rosenberg J.M., Shachar-Hill Y. & Bohnert H.J. (2002) From genome to function: the *Arabidopsis* aquaporins. *Genome Biology*, **3**, 1-17.

Ranathunge K. & Schreiber L. (2011) Water and solute permeabilities of Arabidopsis roots in relation to the amount and composition of aliphatic suberin. *J Exp Bot*, **62**, 1961-1974.

Rodrigues O., Reshetnyak G., Grondin A., Saijo Y., Leonhardt N., Maurel C. & Verdoucq L. (2017) Aquaporins facilitate hydrogen peroxide entry into guard cells to mediate ABA- and pathogen-triggered stomatal closure. *Proceedings of the National Academy of Sciences of the United States of America*, **114**, 9200-9205.

Roppolo D., Boeckmann B., Pfister A., Boutet E., Rubio M.C., Dénervaud-Tendon V., …, Geldner N. (2014) Functional and evolutionary analysis of the casparian strip membrane domain protein family. *Plant Physiology*, **11**, 1709-1722.

Santoni V. (2017) Plant aquaporin posttranslational regulation. Signaling and Communication in Plants - Plant Aquaporins: From Transport to Signaling *François Chaumont, Stephen D. Tyerman ed*, 83-105.

Shahzad Z., Canut M., Tournaire-Roux C., Martiniere A., Boursiac Y., Loudet O. & Maurel C. (2016) A potassium-dependent oxygen sensing pathway regulates plant root hydraulics. *Cell*, **167**, 87-98.

Tornroth-Horsefield S., Wang Y., Hedfalk K., Johanson U., Karlsson M., Tajkhorshid E., …, Kjellbom P. (2006) Structural mechanism of plant aquaporin gating. *Nature*, **439**, 688-694.

Tournaire-Roux C., Sutka M., Javot H., Gout E., Gerbeau P., Luu D.-T., …, Maurel C. (2003) Gating of aquaporins by cytosolic pH regulates root water transport during anoxic stress. *Nature*, **425**, 393-397.

Van Wilder V., Miecielica U., Degand H., Derua R., Waelkens E. & Chaumont F. (2008) Maize plasma membrane aquaporins belonging to the PIP1 and PIP2 subgroups are *in vivo* phosphorylated. *Plant Cell Physiology*, **49**, 1364-1377.

Wu X.N., Sanchez-Rodriguez C., Pertl-Obermeyer H., Obermeyer G. & Schulze W.X. (2013) Sucrose-induced receptor kinase SIRK1 regulates plasma membrane aquaporins in *Arabidopsis*. *Molecular and Cellular Proteomics* **12**, 2856-2873.

Yadav V., Molina I., Ranathunge K., Castillo I.Q., Rothstein S.J. & Reed J.W. (2014) ABCG Transporters Are Required for Suberin and Pollen Wall Extracellular Barriers in Arabidopsis. *Plant Cell*, **26**, 3569-3588.

Zelazny E., Borst J.W., Muylaert M., Batoko H., Hemminga M.A. & Chaumont F. (2007) FRET imaging in living maize cells reveals that plasma membrane aquaporins interact to regulate their subcellular localization. *Proceedings of the National Academy of Sciences (USA)*, **104**, 12359-12364.

Table 1: Characterization of FRET interaction between CASPL1B1, CASPL1D2 and PIP2;1 measured by FLIM.

Average fluorescence lifetimes (τ) of GFP fusion proteins (donor) expressed alone or together with RFP-tagged proteins (acceptor) and corresponding standard error (SE) are given. PIP2;1 was either wild-type (PIP2;1) or with double punctual mutations of Ser280 and Ser283 in Ala (PIP2;1-AA) or in Asp (PIP2;1-DD). N and n correspond to the number of independent experiments and cells measured, respectively.

Donor	Acceptor	τ(ps) ± SE	FRET efficiency	N	n	*p* (Student's *t* test)
GFP-CASPL1B1	-	2296 ± 9	-	4	26	-
GFP-CASPL1B1	RFP-AGG1	2323±11	-1.2%	2	14	$6.78.10^{-2}$
GFP-CASPL1B1	PIP2;1-RFP	2227 ± 10	3.0%	2	14	$1.74.10^{-5}$
GFP-CASPL1B1	PIP2;1-AA-RFP	2219 ± 9	3.3%	2	17	$5.30.10^{-6}$
GFP-CASPL1B1	PIP2;1-DD-RFP	2229 ± 9	2.9%	2	15	$3.97.10^{-5}$
CASPL1D2-GFP	-	2247 ± 12	-	3	23	-
CASPL1D2-GFP	RFP-AGG1	2291±14	-1.9%	1	9	$1.14.10^{-1}$
CASPL1D2-GFP	PIP2;1-SS-RFP	2171 ± 6	1.9%	2	17	$4.40.10^{-4}$

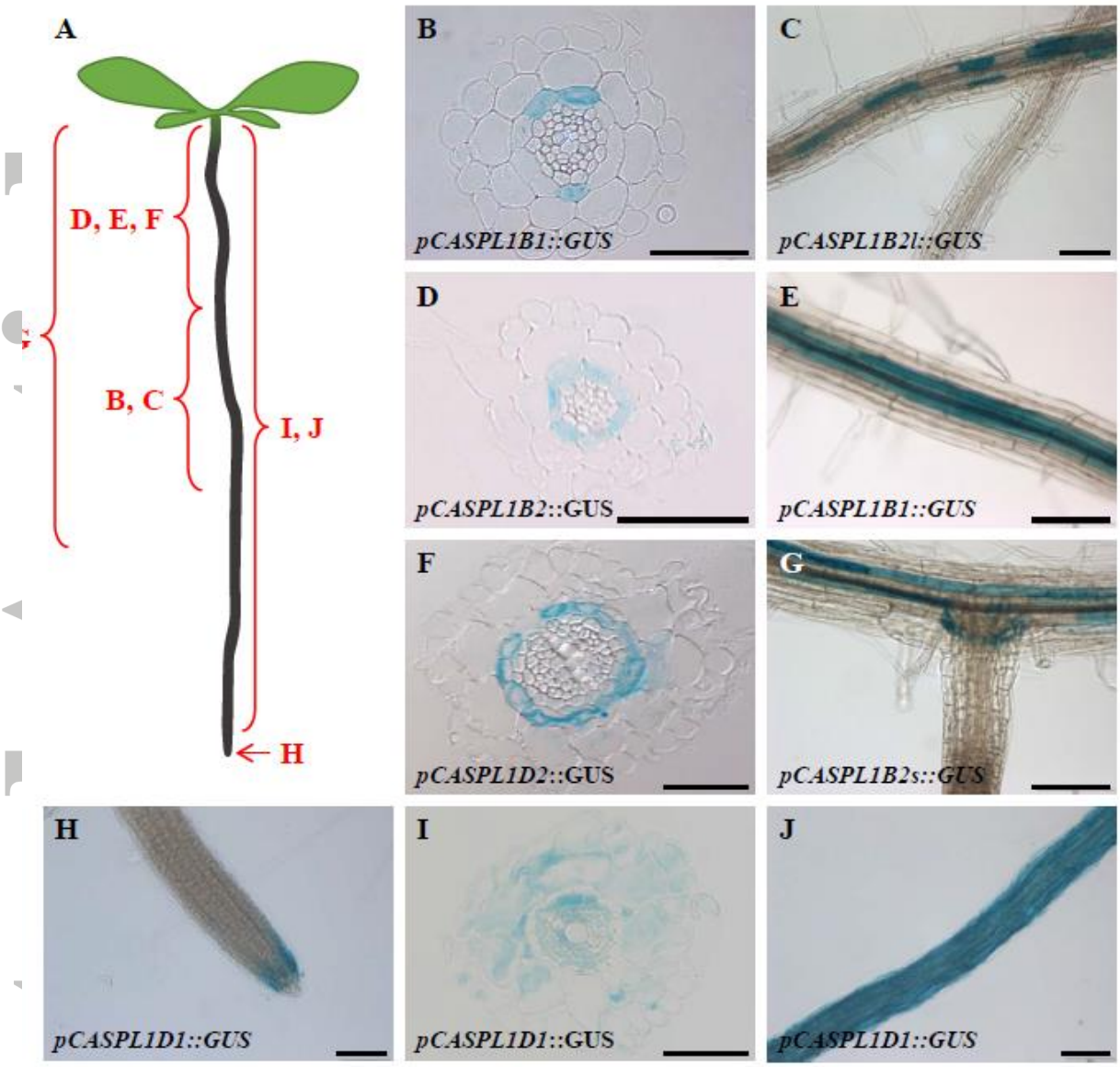

Figure 1 Expression analysis of *CASPL1B1*, *CASPL1B2*, *CASPL1D1* and *CASPL1D2*. GUS staining of 7-8 day-old plants grown *in vitro* and expressing *pCASPL1B1::GUS*, *pCASPL1B2s::GUS*, *pCASPL1B2l::GUS*, *pCASPL1D1::GUS* or *pCASPL1D2::GUS*, as indicated. (a) Schematic representation of the root regions where GUS activity was detected. (b-j) Expression of the indicated GUS constructs in regions depicted in (a). (b-g) The same GUS activity pattern was observed for *pCASPL1B1::GUS*, *pCASPL1B2s::GUS*, *pCASPL1B2l::GUS* and *pCASPL1D2::GUS* constructs. Complementary images are presented in Figure S2. (b), (d), (f) and (i): scale bars = 50 µm; (c), (e), (g), (h) and (j): scale bars = 100 µm.

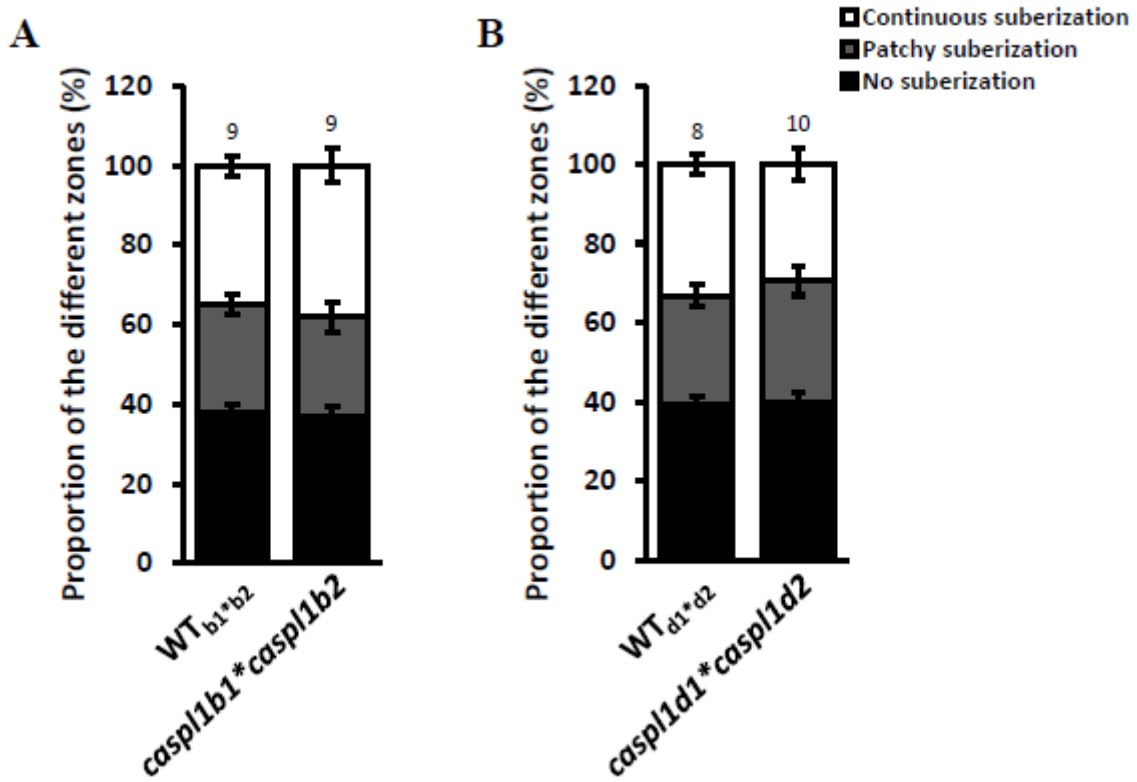

Figure 2 Effect of CASPL1B1, CASPL1B2, CASPL1D1 and CASPL1D2 on suberin deposition. Five day-old plants grown *in vitro* were stained with Fluorol Yellow. The length of the different zones [no suberization (black bars), patchy suberization (gray bars) and continuous suberization (white bars)] is expressed as a percentage of total root length. Two independent biological repeats were performed and the total number of phenotyped plants per genotype is indicated above each bar. The error bars refer to the standard error. For each zone, data from mutant plants were compared to data from control plants by a Student's t test and no difference was detected.

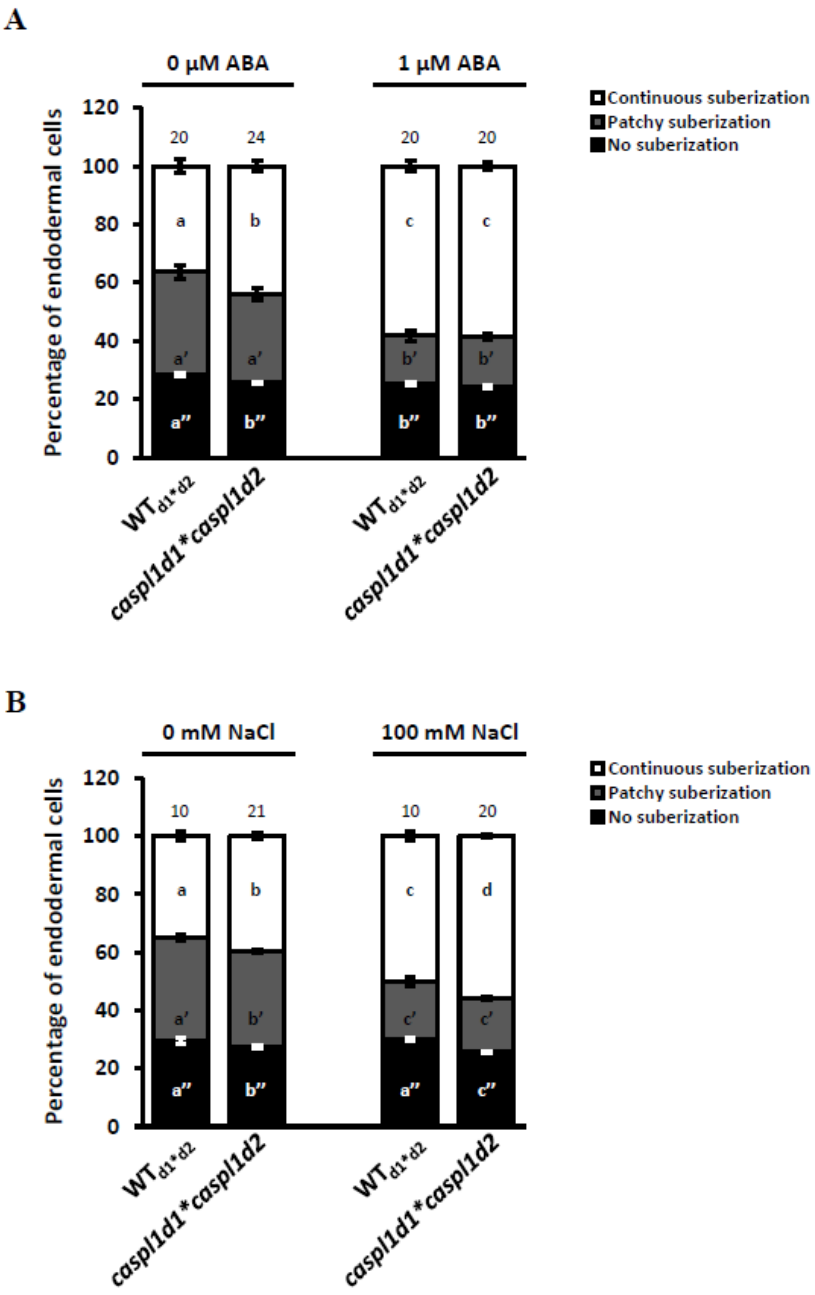

Figure 3 Effect of CASPL1D1 and CASPL1D2 on suberin deposition after ABA (A) or NaCl (B) treatment.

Five-day-old plants were incubated in the presence of 1 µM ABA (A) or 100 mM NaCl (B) for 6hr prior to Fluorol Yellow staining. The different zones [no suberization (black bars), patchy suberization (gray bars) and continuous suberization (white bars)] are expressed as a percentage of total number of endodermal cells. Two independent biological repeats were performed and the total number of phenotyped plants per genotype is indicated above each bar. The error bars refer to the standard error. For each zone, data were compared using one-way ANOVA followed by Newman-Keuls test.

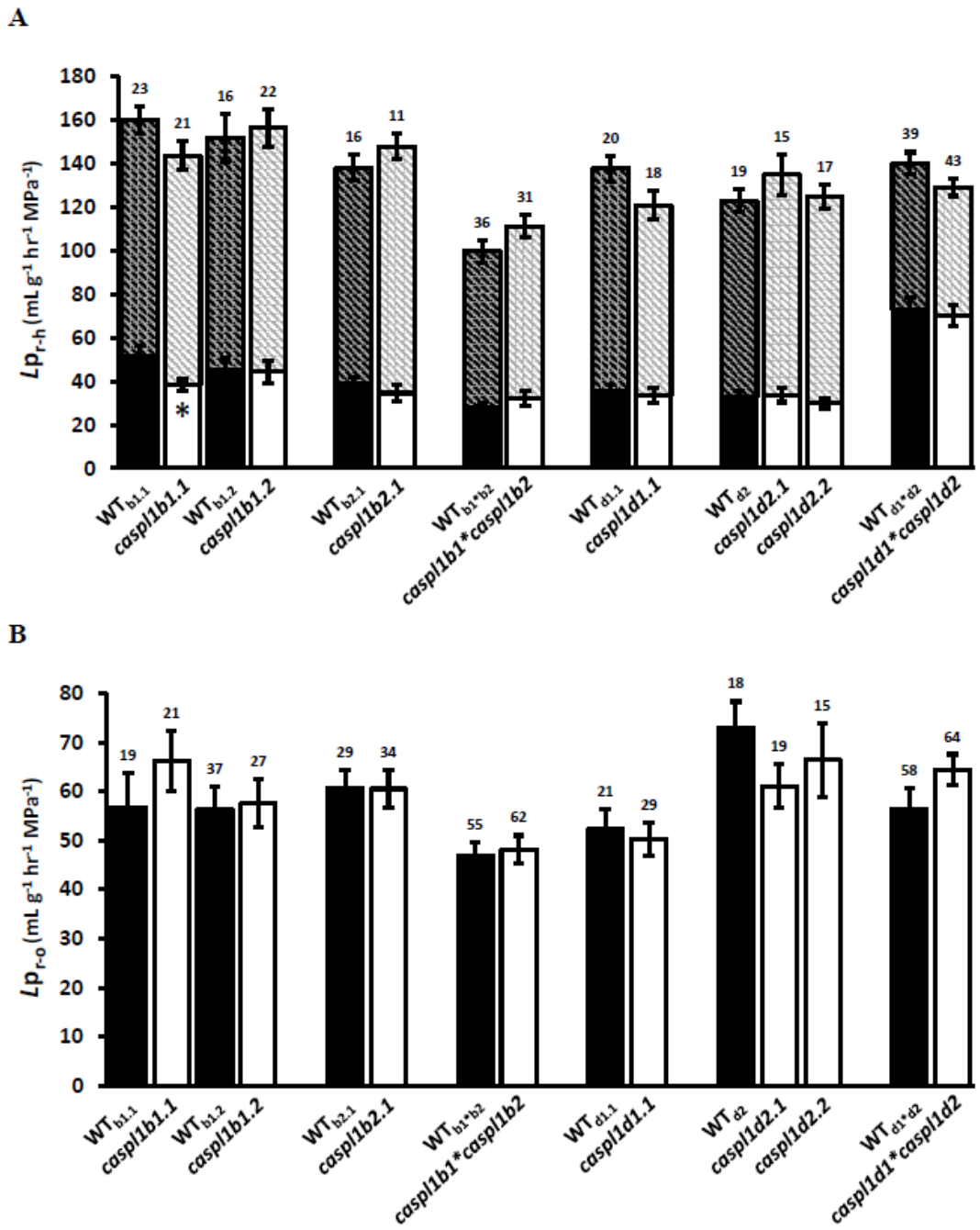

Figure 4 Mean root hydraulic conductivity of *caspl* single and double mutants, and their respective control plants.

Root hydraulic conductivity was measured in pressure chambers (Lp_{r-h}) (A) or by exudation (Lp_{r-o}) (B) on roots of control (black bars) and of mutant (white bars) plants grown in hydroponics. In (A), Lp_{r-h} was measured prior to and after treatment with 1 mM sodium azide. The graph shows the fraction of Lp_{r-h} that is sensitive (hatched bars) or resistant (plain bars) to sodium azide. Two to three independent biological repeats were obtained and the total number of phenotyped plants per genotype is indicated above each bar. The error bars refer to the standard error. Data from mutant plants were compared to corresponding data from control plants by a Student's t test (*: $p \leq 0.05$).

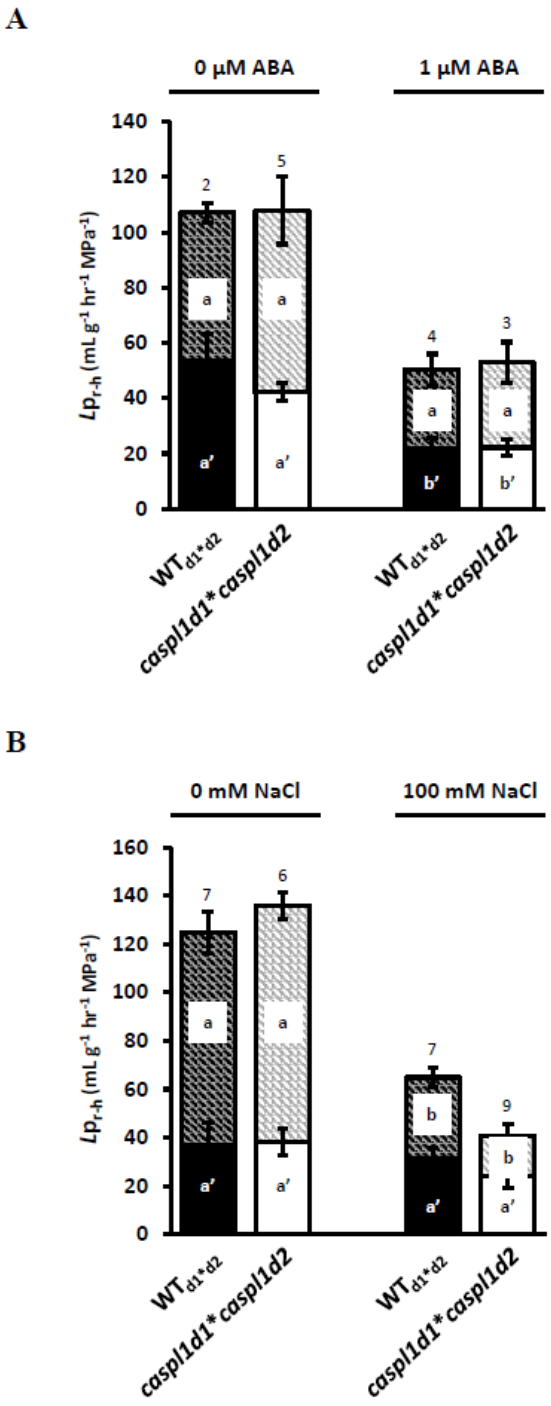

Figure 5 Effect of CASPL1D1 and CASPL1D2 on root hydraulic conductivity after ABA (A) or NaCl (B) treatment.

Root hydraulic conductivity (Lp_{r-h}) was measured in pressure chambers on roots of control (black bars) and mutant (white bars) plants grown in hydroponics and treated with 1 µM ABA (A) or 100 mM NaCl (B) for 6hr. Lp_{r-h} was measured prior to and after treatment with 1 mM sodium azide. The graph shows the fraction of Lp_{r-h} that is sensitive (hatched bars) or resistant (plain bars) to sodium azide. Two independent biological repeats were performed and the total number of phenotyped plants per genotype is indicated above each bar. The error bars refer to the standard error. Data were compared using one-way ANOVA followed by Newman-Keuls test.

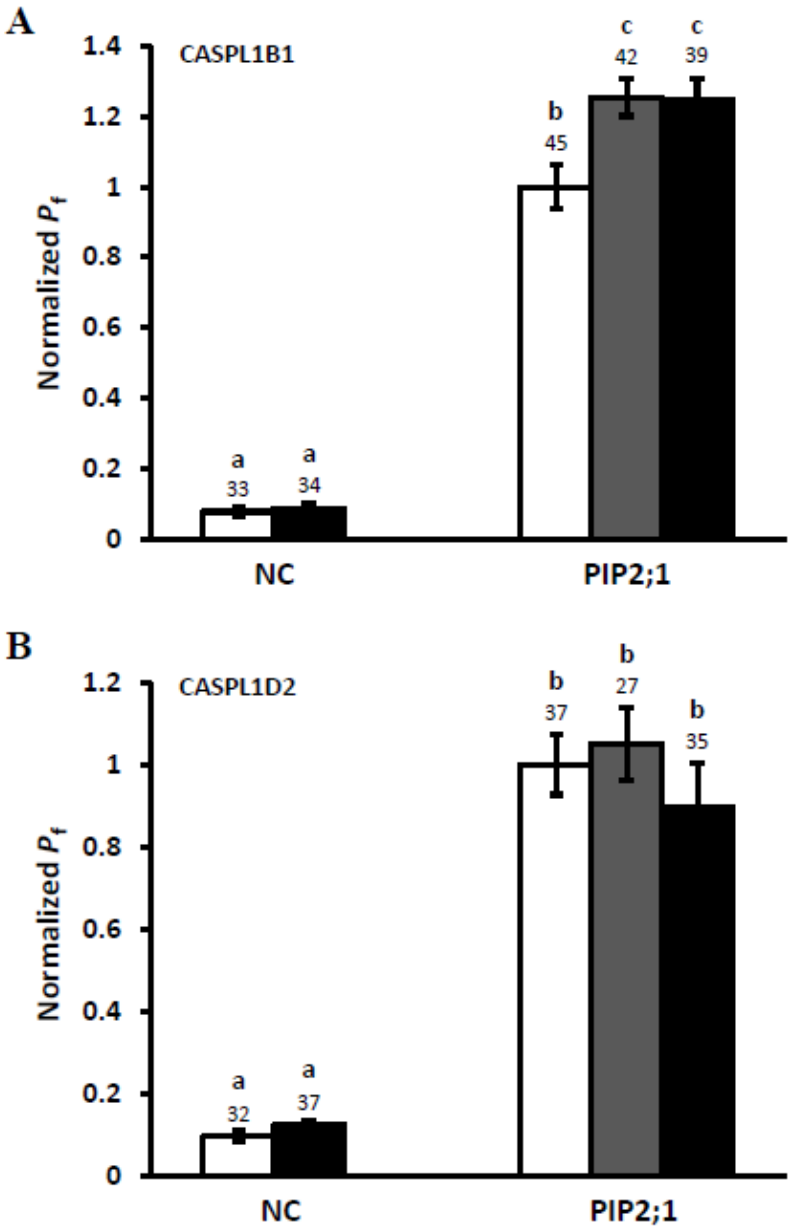

Figure 6 Functional co-expression in Xenopus oocytes of PIP2;1 with CASPL1B1 (A) and CASPL1D2 (B).

Oocytes were injected with cRNAs as indicated: (A) 5 ng (grey bars) or 15 ng (black bars) of CASPL1B1 cRNA with 10 ng of PIP2;1 cRNA; (B) 5 ng (grey bars) or 15 ng (black bars) of CASPL1D2 cRNA with 10 ng of PIP2;1 cRNA. Uninjected oocytes (NC, white bars) and oocytes injected with 15 ng of CASPL cRNA (NC, black bars) were used as negative controls for oocytes injected with PIP2;1 cRNA (PIP2;1, white bars) or co-injected with PIP2;1 cRNA and CASPL cRNA (PIP2;1, grey and black bars), respectively. P_f was measured 3-4 days after injection and, for each of the 3 independent biological repeats, P_f data were normalized with regard to the mean P_f of oocytes injected with PIP2;1 cRNA alone [(A): 131, 286 and 281 µm s^{-1} and (B): 131, 259 and 170 µm s^{-1} for the 3 independent biological repeats]. The total number of oocytes measured per condition is indicated above each error bar referring to the standard error. P_f data were compared using one-way ANOVA followed by Newman-Keuls test.

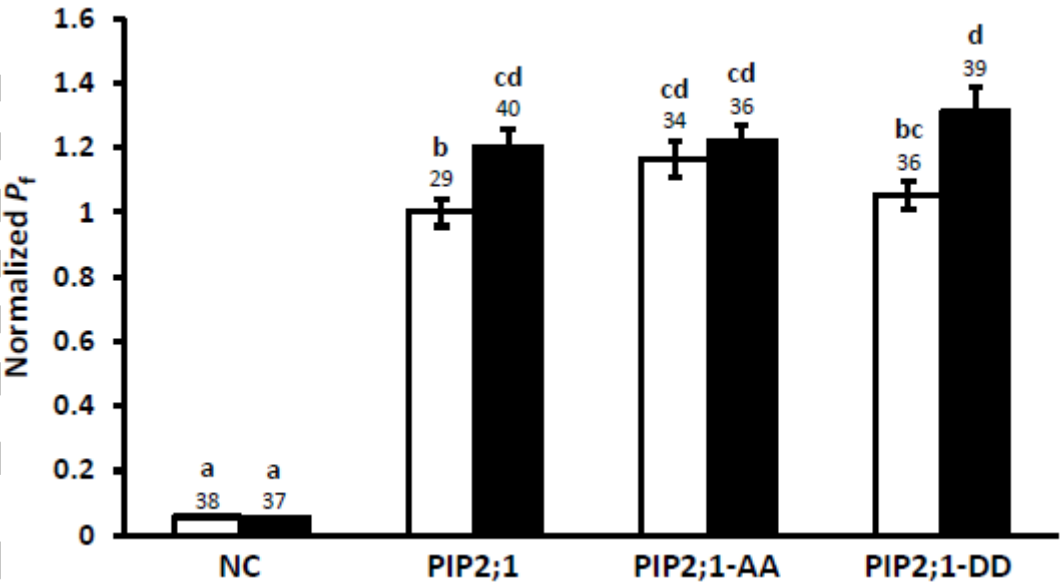

Figure 7 Functional co-expression in Xenopus oocytes of CASPL1B1 with different forms of PIP2;1.

Oocytes were injected with 3 ng of CASPL1B1 cRNA (black bars) and 1 ng of cRNA of the wild-type form of PIP2;1 or PIP2;1 forms with Ser-to-Ala (PIP2;1-AA) or Ser-to-Asp (PIP2;1-DD) mutations at positions 280 and 283. Uninjected oocytes (NC, white bars) and oocytes injected with 3 ng of CASPL1B1 cRNA (NC, black bars) were used as negative controls for oocytes injected with cRNA of the different PIP2;1 forms cRNA (PIP2;1, PIP2;1-AA and PIP2;1-DD, white bars) or co-injected with cRNA of the different PIP2;1 forms and CASPL1B1 cRNA (PIP2;1, PIP2;1-AA and PIP2;1-DD, black bars) respectively. P_f was measured 4 days after injection and, for each of the 3 independent biological repeats, P_f data were normalized with regard to the mean P_f of oocytes injected with PIP2;1 cRNA alone (186, 157 and 193 µm s^{-1} for the 3 independent biological repeats). The total number of oocytes measured per condition is indicated above each error bar referring to the standard error. P_f data were compared using one-way ANOVA followed by Newman-Keuls test.